Towards functional annotation with latent protein language model features

Jake Silberg [*1] **Elana Simon** [*1] **James Zou** [1]

Abstract

Protein Language Models (PLMs) create high-dimensional embeddings that can be transformed into interpretable sparse features using Sparse Autoencoders (SAEs), where each feature activates on specific protein elements or patterns. However, scalably identifying which features are cohesive and reliable enough for protein annotation remains challenging. We address this by developing a validation pipeline combining three complementary methods: (1) expanded database matching across 20+ annotation sources including hierarchical codes, (2) feature-guided local structural alignment to identify structurally consistent activation regions, and (3) LLM-based feature description generation. Our annotation pipeline demonstrates three key properties of SAE features that make them a useful source of functional annotation complementary to existing methods. First, they can represent more granular patterns than existing protein databases, enabling the identification of sub-domains within proteins. Second, they can detect missing annotations by finding proteins that display recognizable structural motifs but lack corresponding database labels. Here, we automatically identify at least 491 missing CATH topology annotations with our pipeline. Third, they can maintain structural consistency across unseen proteins. Of our 10,240 SAE features, we find 615 that are consistently structurally similar in unannotated metagenomic proteins, allowing us to structurally match at least 8,077 metagenomic proteins to characterized proteins. This provides a rapid annotation pipeline with constant time search regardless of database size, that automatically includes structural and function information about the feature that triggered the match.

[*]Equal contribution [1]Department of Biomedical Data Science, Stanford University. Correspondence to: Jake Silberg <jsilberg@stanford.edu>.

Proceedings of the Workshop on Generative AI for Biology at the 42nd International Conference on Machine Learning, Vancouver, Canada. PMLR 267, 2025.

1. Introduction

Proteins play essential roles in nearly all biological processes, yet our ability to annotate their functional elements lags behind recent growth in sequence data. With the advent of metagenomics, vast datasets of protein sequences have been identified, but many remain functionally uncharacterized (Karin & Steinegger, 2025). Traditional computational methods annotate proteins based on similarity to well-characterized peers, but these approaches struggle when sequence similarity is low (Karin & Steinegger, 2025).

Recent advances in protein language models (PLMs) like ESM-2 (Lin et al., 2023) have demonstrated remarkable ability to capture evolutionary patterns across the protein universe. However, ESM embeddings cannot easily be translated into interpretable features that represent specific protein domains. Sparse autoencoders (SAEs) have emerged as powerful tools for mechanistic interpretability, and when applied to PLMs, they can decompose dense embeddings into interpretable features that frequently correspond to functional protein elements without biological supervision (Simon & Zou, 2024), (Adams et al., 2025). This remarkable correspondence suggests that SAE features could serve as a foundation for efficient functional annotation.

However, not all SAE features are suitable for annotation. Some may be polysemantic, activating on multiple unrelated concepts, while others may represent patterns meaningful to the model but not interpretable by humans who rely on structural, sequential, and functional annotations.

To harness SAE features for practical annotation, we need to systematically identify features that correspond to interpretable biological concepts. To identify cohesive features, we focus on those that activate most strongly on groups of proteins that are functionally or structurally related, as defined by meeting one of three validation criteria:

1. A single annotation from an existing annotation database is predictive of feature activation
2. The activating regions of the highest activating proteins are structurally similar
3. A language model can generate a feature description that is predictive of activation, as validated in a held-out set of proteins

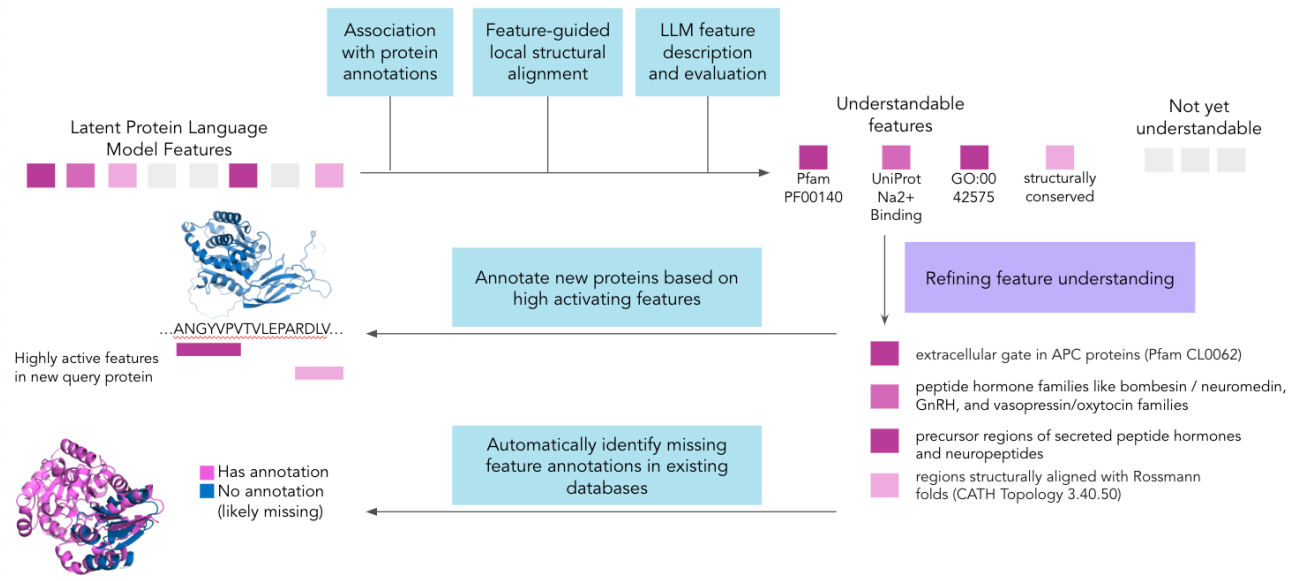

Figure 1. Workflow for protein-latent feature applications.

In this work, we analyze latent features from an SAE trained on Layer 18 of ESM-2 650M, yielding 10,240 features (referred to throughout as f/feature-number, e.g., f/401). This layer was chosen as it sits in the middle of ESM, similar to natural language LLM SAE work that focused on middle layers (Templeton et al., 2024). Our analysis proceeds in two main parts. First, we develop and evaluate our three-pronged validation approach, demonstrating how expanded database matching, feature-guided local structural alignment, and LLM-based pattern recognition complement each other to identify cohesive features. We show this approach doubles annotation coverage, identifying over 60% of features with strong correspondence to biological annotations ($F1 > 0.8$), based on sampling 1000 of our features. With local structural alignment, we find an additional 2.4% of the features with worse correspondence to existing databases, but high structural similarity.

Second, we demonstrate three practical applications that highlight the unique advantages of SAE features for protein annotation: (1) capturing granular subdomains within existing annotations that reveal discrete functional units, (2) detecting missing annotations by identifying proteins with recognizable structural motifs that lack corresponding database labels, and (3) enabling zero-shot generalization to novel metagenomic proteins, including those without matches to existing protein families, specifically, Pfam (Bateman et al., 2004).

Utilizing PLM SAE features in this annotation pipeline offers natural advantages: First, because the top structures for each feature can be pre-computed, during a search, hits can be found in constant-time search regardless of database size. Second, because we know the feature(s) triggering the hit, the search can automatically include known structural or functional information about that feature (such as its links to existing databases or a natural language description). Finally, because the features are found in an unsupervised manner, the search can find structural hits based on features not in existing databases.

2. Related Work

Traditional Sequence-Based Annotation Methods

Functional annotation of uncharacterized proteins has historically relied on sequence conservation approaches. Hidden Markov Models and Position-Specific Scoring Matrices form the foundation of major databases including CATH (Orengo et al., 1997) via Gene3D (Buchan et al., 2002) and Pfam (Bateman et al., 2004). These have been integrated into unified resources like UniProt (Consortium, 2015) and InterPro (Hunter et al., 2009), with search tools like InterProScan enabling annotation of arbitrary sequences (Jones et al., 2014). However, these methods struggle with divergent sequences, particularly from metagenomic sources, leading to specialized databases like Novel Metagenomic Pfams (NMPfamsDB) (Baltoumas et al., 2024) that specifically curate sequences lacking Pfam annotations.

Structure-Based Approaches

The advent of AlphaFold 2 (Jumper et al., 2021) has catalyzed a shift toward 3D structure-based annotation methods.

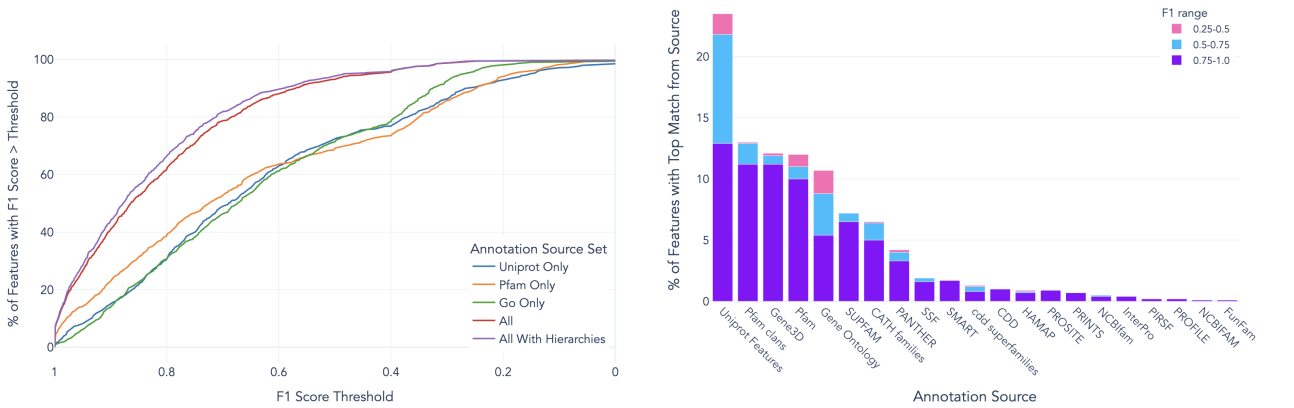

(a) Percentage of features that match existing database annotations, by sources of annotations, for 1000 sampled features.

(b) Distribution of the common sources of the top annotation match per feature (highest feature F1 score) for 1000 sampled features.

Figure 2. We find additional databases greatly expand our ability to find cohesive features. Hierarchical codes like Pfam clans often correspond more closely to a feature than any individual Pfam code, indicating the SAE learns features at different levels of specificity.

This has enabled new databases focused on structural similarity, such as the Encyclopedia of Domains (Lau et al., 2024) based on the Merizo tool (Lau et al., 2023). However, large-scale structural searching remains computationally challenging despite algorithmic advances like TMalign (Zhang & Skolnick, 2005) and CEalign (Shindyalov & Bourne, 1998). FoldSeek addresses this by converting structural similarity search into sequence matching using a 3D-informed alphabet, achieving orders-of-magnitude speedup (van Kempen et al., 2022). Merizo-search uses embeddings trained on CATH domains for rapid structural matching (Kandathil et al., 2025). While powerful, these approaches have limitations: FoldSeek doesn't automatically provide domain-specific functional information about the region(s) of each protein that triggered the match, and Merizo-search is constrained to identify hits based on supervised training on CATH annotations.

Interpretable Features from Protein Language Models

Recent work has begun exploring sparse autoencoders (SAEs) for extracting interpretable features from protein language models. InterPLM (Simon & Zou, 2024) demonstrated correspondence between individual amino acid activations and UniProtKB annotations, while InterProt (Adams et al., 2025) associated protein-level SAE activations with Pfam families. However, these approaches achieved limited coverage, leaving over 75% of features unexplained when using stringent matching criteria.

Our work extends this foundation by: (1) incorporating the full InterPro database across 20+ annotation sources including hierarchical codes, (2) developing systematic structural validation through feature-guided local structural alignment, and (3) integrating LLM-based pattern recognition to identify features missed by existing databases. This comprehensive approach doubles annotation coverage while enabling practical applications for both missing annotation detection and novel protein characterization.

3. Using existing database annotations, local structural alignment, and LLMs to screen SAE features for cohesiveness

3.1. Combining protein annotation databases identifies structurally and functionally cohesive features

We expand annotation coverage by incorporating the full InterPro database (Hunter et al., 2009), which includes annotations from UniProtKB, Pfam, CATH / Gene3D (Orengo et al., 1997), (Buchan et al., 2002), and 19 other sources. We evaluate associations at the protein level rather than amino acid level, allowing us to capture cases where feature activations occur near—but not exactly on—annotated elements, and enabling us to combine both protein-level annotations (like Pfam domains) and more granular annotations (like binding sites and motifs in UniProtKB). We also include hierarchical codes such as Pfam clans and CATH topologies to capture broader biological concepts.

For each SAE feature, we sample up to 1100 proteins across 10 activation levels (up to 100 proteins each for activation 0, 0.1, etc up to 1.0) and test whether any single annotation code can predict high versus low feature activation, calculating F1 scores between predicted and actual activations. **This approach doubles our annotation coverage.** As shown in Figure 2, expanding beyond single databases increases the percentage of features with F1 $>$ 0.8 from approximately 25% to over 60%. The highest-performing features

are distributed relatively evenly across UniProtKB annotations, Pfam clans, Gene3D/CATH codes, and individual Pfam families, demonstrating that SAE features capture biological concepts at multiple levels of granularity. Features with moderate performance (F1 0.5-0.75) are predominantly associated with UniProtKB categories.

This metric serves dual purposes: quantifying annotation correspondence and screening for feature cohesiveness—features that correspond strongly to existing annotations likely represent understandable biological elements suitable for annotation purposes.

3.2. Feature-guided local structural alignment independently identifies structurally cohesive features

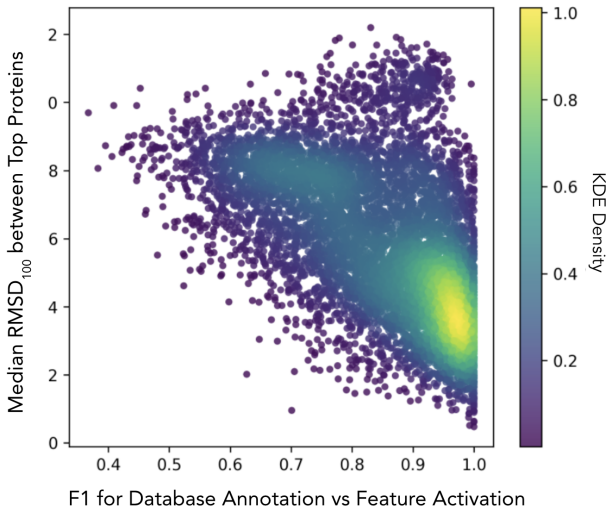

Figure 3. RMSD vs. F1 for existing database annotations. Many features with high $RMSD_{100}$ do not correspond closely with existing annotations, while the vast majority of features with low $RMSD_{100}$ correspond with existing database annotations.

To better understand what causes these features to fire, we turn to structural analysis. This serves two benefits. First, we can track structural subdomains that may not have their own annotation. Second, we can track structural elements that fire even when an annotation is missing. InterPLM (Simon & Zou, 2024) demonstrated that when a feature associated with an existing annotation activates on a protein that lacks this corresponding annotation, what initially appears to be an erroneous feature activation can actually indicate missing or incorrect database labels. Through manual inspection, they identified three features that were correctly identifying functional patterns in proteins that should have been annotated but weren't. However, investigating each feature individually for missing labels through manual verification would be infeasible at scale, motivating our automated pipeline for systematically identifying such annotation gaps.

To scale up this process, we introduce a procedure for Feature-Guided Local Structural Alignment to find "structurally cohesive" features, meaning the regions that activate highly have a consistent 3D structure, even if it has not necessarily been annotated. In our procedure, we sample 20 AlphaFold-predicted structures from the top activating proteins of a given SAE feature (activation above 0.7), after de-duplicating for structures from gene orthologs. We then crop all selected structures to the 100 amino acids surrounding the peak activating SAE amino acid. We run pairwise local alignment between all possible pairs, and score the alignments with backbone $RMSD_{100}$, a modification of Root Mean Square Deviation that allows for more lenience for longer alignments (Carugo & Pongor, 2001). We use this rather than RMSD because it advantages longer alignments, finding more complex conserved structures rather than, for example, a single alpha helix match. Because we are only aligning cropped structures, we can use a robust structural alignment algorithm, CEalign (Shindyalov & Bourne, 1998) with minimal cost. Additionally, by restricting alignments to regions where the SAE feature activates, this procedure ensures we evaluate structural similarity in functionally relevant areas.

In Figure 3 we see that better structural alignment (lower $RMSD_{100}$) is correlated (pearson r=0.53) with higher annotation code F1 scores. Specifically, 92% of features with $RMSD_{100} < 5$ have a code-based F1 $> .8$, while only 51% of features with an $RMSD_{100} > 5$ have a code-based F1 $> .8$. This helps serve as a filter for feature cohesiveness. That is, for pairwise alignments with low $RMSD_{100}$, we would expect they indeed share a local structural feature, even if one protein is missing an annotation, or is an uncharacterized novel protein. Since $RMSD_{100}$ scores below 4 consistently indicate clear structural similarity, we use this as our stringent threshold. Scores between 4 and 5 also typically represent genuine structural similarity but with some false positives, making this our more permissive threshold for broader coverage.

3.3. Large Language Models identify additional cohesive features missed by other methods

While many features fire on a single existing database annotation code, other features appear to fire on shared traits across existing annotations. Thus, asking LLMs to reason over protein data is a natural step in developing better feature descriptions that can be used for protein annotation. We adapt the automated pipeline from InterPLM (Simon & Zou, 2024), using Claude-3.5 Sonnet (New) to generate feature descriptions by providing it with protein metadata from our expanded annotation sources along with examples of 40 proteins showing varying levels of maximum feature activation. The LLM analyzes these examples to identify what protein and amino acid characteristics cause the feature to activate

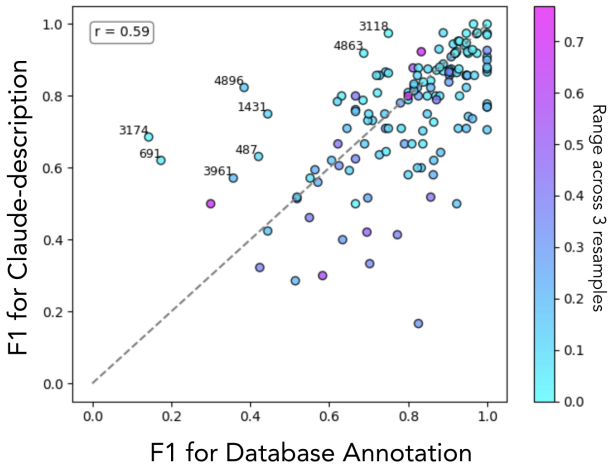

Figure 4. LLM-based F1 score vs. annotation code-based F1 score on the same train/val split.

at different levels, generating natural language descriptions of the underlying biological patterns.

As validation, we test whether these LLM-generated descriptions can predict feature activation levels on held-out proteins. We evaluate the ability of both the generated descriptions and the expanded annotation metadata to classify proteins as high or low activating for each feature, calculating F1 scores on a separate test set to ensure the descriptions capture generalizable patterns rather than overfitting to the training examples.

We find that the LLM's ability to describe a feature is highly correlated with the F1 score of the single best annotation code, as shown in Figure 4. That is, though we want the model to reason about a combination of codes, a primary driver of performance is the primary existing database annotation.

Still, we find interesting cases where the LLM quantitatively improves performance. For example, for one of our features, noted as f/3174, the LLM identifies "this feature activates on transmembrane domains in multi-pass membrane proteins, particularly those involved in protein complex assembly and ion transport across membranes." This description, which focuses on transmembrane domains across a broader range of proteins than would be covered by a single Pfam family or clan, allows the description to outperform existing annotation codes. Similarly, for another feature (f/4896), the LLM writes, "This feature activates on precursor regions of secreted peptide hormones and neuropeptides that undergo proteolytic processing to produce bioactive signaling molecules." This LLM description correctly identifies that the feature fires on several different types of peptide hormones and neuropeptides, even though they do not share a GO code.

Finally, the LLM can sometimes still interpret polysemantic features that appear to fire on two distinct protein elements. For example, f/3118 appears to fire at both the phosphohistidine of histidine kinases, and at chlorine channel sites for proton-coupled chloride transporters. While we have not been able to find a sequential or structural similarity between these two kinds of sites, the LLM correctly describes that the feature, "activates on functional domains involved in ion-mediated signaling, particularly histidine kinase domains and chloride channel domains that facilitate ion transport across membranes." Thus, the LLM description is consistently able to get a nearly perfect predictive F1. Ideally this feature would fire on a single monosemantic concept, and this demonstrates room for improvement in the SAE and limitations of using this F1 score to identify purely monosemantic concepts. However, this description can still help us with feature annotation as it reveals that the activating proteins are likely one of two connected types that function in a similar pathway.

We also analyze the 21 cases from our sampled features where the code-based F1 is at least .2 or more higher than the LLM-generated description's F1, that is, the LLM underperformed. In 20 of these cases, we find that precision was higher than recall. In fact, in 17 of the 21, precision was higher than .8 while for only 1 of the 21 cases was recall higher than .8. This indicates that the LLM is sometimes writing overly specific descriptions, so it is missing a broader view of what causes the feature to activate. For example, for f/657, the description is "This feature activates on catalytic domains of intradiol ring-cleavage dioxygenases and carboxypeptidases," which achieves an F1 of 0.5, but a precision of .875. The description is missing other elements besides these that also cause the feature to fire. In fact, this feature is highly associated with the Pfam clan CL0287, 7 stranded beta sandwiches. This does potentially point a way forward for the LLMs. Their focus is likely driven by having too few examples in order to fit into the context window. This suggests additional activating examples might help them identify the broadest possible applicable description.

4. Using PLM SAE features to enhance protein annotation

Having identified cohesive features using our three approaches, we now show three benefits of utilizing these features. In particular, we utilize these features to identify discernible subdomains within existing annotations that have been specifically researched in the literature. Second, we utilize these features to scalably identify missing CATH annotations. Finally, we utilize these features to rapidly identify structural matches for unseen metagenomic proteins in NMPfamsDB.

4.1. SAE features capture granular subdomains interpretable through targeted literature search

While our annotation matching successfully identifies coherent features, it also reveals an important limitation: we can identify the **types** of proteins where features activate, but not always what **specific elements within** those proteins cause the activation. This limitation, however, highlights a key advantage of SAE features—their ability to capture functional granularity beyond existing annotation schemes. Multiple distinct SAE features often share the same top annotation code yet activate on different structural subregions, revealing functional subdomains that current databases treat as single units.

Figure 5 illustrates both this limitation and opportunity. Eight different features (f/253, f/515, f/1505, f/1579, f/1712, f/1731, f/2768, and f/3288) all achieve high F1 scores for the same Pfam clan annotation (APC clan, CL0062), yet each activates on distinct protein regions—different transmembrane alpha helices, cytoplasmic domains (f/253), and extracellular domains (f/515). While our annotation-based screening identifies these as coherent features, it cannot explain their specific functional roles, demonstrating both the power of SAE features to decompose protein families and the need for methods to interpret this finer granularity.

To bridge this gap, we tested whether language models could automatically retrieve literature discussing the specific protein regions where features activate. We provided OpenAI's o4-mini-high with the 10 highest-activating proteins for selected features, their gene descriptions from UniProtKB, and precise amino acid positions of peak activation, asking it to search for literature describing these specific regions.

In a pilot evaluation of 6 features, this approach successfully identified papers that discussed the exact regions highlighted by our features for 4 cases. For example, for f/515, the model retrieved literature on extracellular loops in APC proteins, identifying the effects of mutations in this precise extracellular gating region (Raba et al., 2014)—functional detail entirely absent from the broader clan annotation. An example prompt for this pilot, and more detail on the retrieved papers is in Appendix B.

This demonstrates that SAE features can reveal biologically meaningful subdomains within existing annotations, but realizing this potential requires methods to interpret their specific functional roles. While literature search shows promise for this task, it currently requires manual validation and is limited by API availability. As these capabilities improve, they could enable systematic annotation of the functional subdomains that SAE features uniquely capture.

4.2. SAE features can identify missingness in existing databases

Our local alignment procedure can specifically analyze features that appear better conserved structurally than their database annotations would suggest. Specifically, we examine proteins that all activate the same SAE feature but differ in their annotation status—some have the expected database annotation while others do not. When we measure $RMSD_{100}$ between annotated and unannotated proteins, we often find they align just as well structurally as annotated proteins align with each other, as shown in Figure 6. This suggests the unannotated proteins may have missing database labels despite possessing the same structural motif.

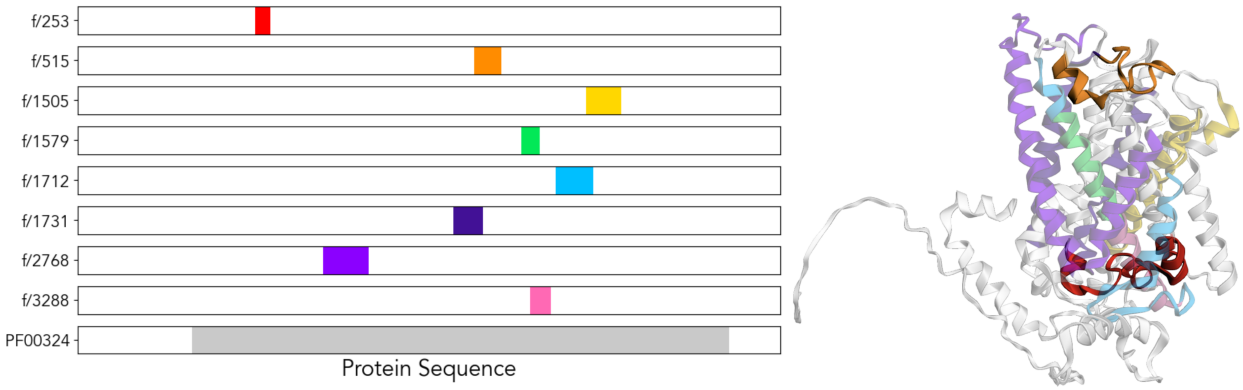

Figure 5. Eight SAE features correspond to the same Pfam clan (APC, CL0062) but activate on distinct structural components within GAP1_YEAST, including different transmembrane helices, cytoplasmic domains, and extracellular loops. Left: Each row shows feature activation along the protein sequence with highly activated (> 0.8) residues highlighted in color, compared to the single Pfam domain (gray). Right: Feature activations on AlphaFold predicted structure (AFDB: P19145) showing each feature highlighting distinct structural components.

For example, we note f/401, whose best code-based description is that it fires on a CATH Topology (3.40.50) with F1 of .84. However, several of the top activating proteins for f/401 in our dataset are not tagged with any CATH code using Gene3D. Still, these structures have very low local RMSD's to structures that are tagged with the CATH code using Gene3D, as shown in the figure, suggesting the CATH code is missing.

To analyze this at scale, we reviewed the 20 proteins per feature randomly sampled in Section 3.2, looking at features with a code-based F1 of .8 or above for a CATH code or CATH topology. Across 221 features, we find 1,055 of those top activating proteins in Swiss-Prot that are not tagged with a CATH code by Gene3D, but have strong local structural similarity to a protein for that feature that does have a Gene3D annotation.

As external validation, we then compare the CATH tags from Gene3D, a sequence-based model, to TED (Lau et al., 2024), which uses a deep learning structure-based approach. We find that 491 of these proteins indeed do have a hit for that same CATH topology in TED (see Appendix Table 2). For proteins that do not have hits even in TED, it is possible that these features can fire on a subdomain within a CATH code, though the entire structure is not similar enough to be tagged.

While we can verify these seemingly missing annotations for CATH by using TED, there are SAE features that align with annotations from other databases like Pfam or UniProtKB. Thus, this combination of screening for existing annotations and local structural alignment can likely help identify potential missing annotations beyond just CATH.

4.3. Features can rapidly detect structural matches in unannotated metagenomic proteins

A key advantage of feature-based annotation is that granular features can detect conserved domains even when full proteins show no sequence similarity to known families. This enables annotation of highly divergent metagenomic sequences that lack Pfam matches, which we test using NMPfamsDB (Baltoumas et al., 2024), a collection of metagenomic proteins that do not have any Pfam matches.

We find that many of our features activate highly in proteins the SAE was not trained on. Specifically, for over 50% of our features, there is at least one NMPfamsDB protein that activates that feature with a value ≥ 0.7. Then, by applying our local structural alignment procedure, we can identify 615 features with strong median local structural alignments ($RMSD_{100} < 5$ for pairwise alignments between one Swiss-Prot protein and one metagenomic protein) and 181 features with median $RMSD_{100} < 4$. This is strong evidence these features activate on the same structural element in both Swiss-Prot proteins and metagenomic proteins, as seen in Figure 7.

In total using just these 615 features, we find matches between 12,526 metagenomic proteins in NMPfamsDB and Swiss-Prot proteins with an $RMSD_{100} \leq 5$ (14.9% of the 83,878 metagenomic proteins in NMPfamsDB we analyzed). At an $RMSD_{100}$ threshold of 4 or better, we can find matches for 8,077 metagenomic proteins (9.6%).

Perhaps unsurprisingly, many of the SAE features that align structurally in the metagenomic proteins also have high correspondence to CATH domains (378 of the 615 have a code-based F1 above 0.8 for a CATH code). This further highlights the importance of a high sensitivity approach discussed earlier.

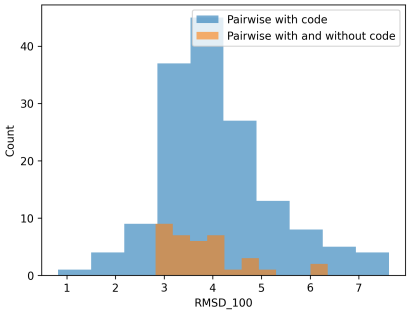

(a) Histogram for f/401 of $RMSD_{100}$ for pairwise alignments

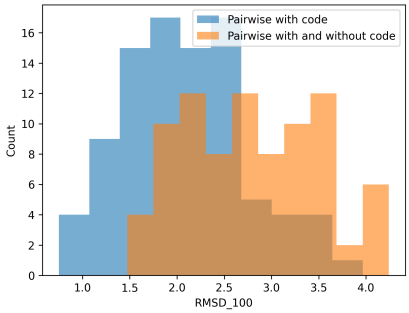

(b) Histogram for f/581 of $RMSD_{100}$ for pairwise alignments

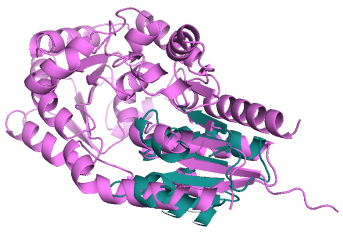

(c) Alignment for proteins with and without CATH 3.4.50.

Figure 6. Aligning structures with the top existing annotation to structures without the annotation reveals features like (a) f/401 and (b) f/581 with strong structural similarity despite different annotations. This can identify missing annotations in existing databases, like in (c) showing an alignment for two proteins that activate on f/401 where one protein (Q0P9A8) has and one protein (Q5WSK6) is missing the CATH 3.40.50 annotation, the topology code for the Rossmann fold. For clarity, only the area around the feature is shown for Q5WSK6.

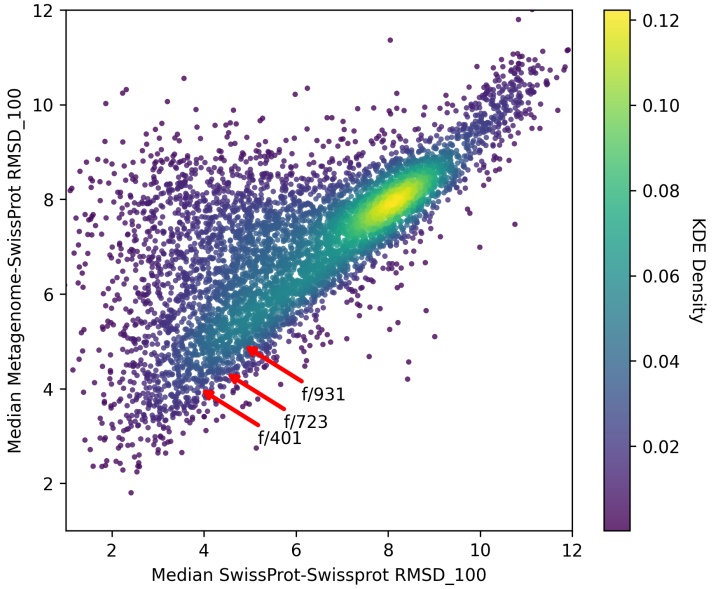

(a) Median $RMSD_{100}$ per feature, for comparisons within UniProt or between UniProt and metagenomic proteins

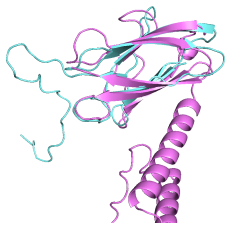

(b) Q9M9H7 (Swiss-Prot) and F014369 (NMPfamsDB). Both activate on f/931.

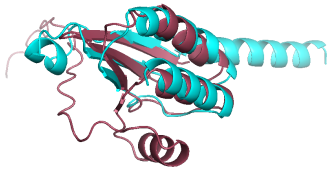

(c) O06984 (Swiss-Prot) and F001558 (NMPfamsDB). Both activate on f/723.

Figure 7. (a) $RMSD_{100}$ for comparisons within Swiss-Prot or between Swiss-Prot and metagenomic proteins; (b) local structural alignment for f/931 for a Swiss-Prot (Q9M9H7) and metagenomic protein F014369; (c) local structural alignment for f/723 for a Swiss-Prot (O06984) and metagenomic protein F001558.

Still, we also find additional features like f/723 and f/931 that correspond to a granular sub-domain within Pfam codes, even though full domain Pfam hits have been screened out of NMPfamsDB. As a final corroboration, for f/723 and f/931, we note that for several metagenomic proteins, if we run FoldSeek on the protein, several of the top Swiss-Prot hits also activate on our SAE feature. That demonstrates that, for the proteins we trained on, these SAE features can be used to find the same structural element found by FoldSeek. However, using SAE features has a natural advantage over FoldSeek, in that we can automatically provide the known structural or functional information about the features that triggered the alignment.

5. Conclusion

In this work, we demonstrate the potential benefits of using latent features from protein language models for protein annotation. We find features that consistently activate on local, discernible elements of proteins, though this cannot yet be understood automatically. We also find features that can identify missing database annotations at scale, and find features that allow us to characterize unseen, unannotated metagenomic proteins. We can pre-compute the top proteins for each feature, tie each feature to existing databases, and generate LLM-descriptions. Thus, for a novel protein, this workflow returns not only a structurally similar characterized protein, but also structural or functional information about exactly the aligned region. This framework provides a scalable annotation solution with unique computational properties: O(1) search time, interpretable matches, and subdomain-level sensitivity.

We note several important limitations of the work: first, while LLMs can help in pulling relevant literature, identifying where within proteins these features fire remains primarily a manual task due to hallucinations and the need for careful verification. Second, our structural validation approach requires conservation within 100 amino acids of peak activation, which likely misses features that span multiple distant regions or involve flexible structural motifs. Third, for now we rely on a single layer (Layer 18) of ESM-2 650M and focus our annotation validation on Swiss-Prot proteins, which increases the density of annotations within structural matches but limits the space of proteins we can match.

Future work should expand analysis across multiple layers within protein language models, test on more powerful protein embedding models, and systematically evaluate how the quality of the latent features influences our ability to find structurally consistent matches. Additionally, more rigorous benchmarking against existing annotation approaches like FoldSeek and Merizo-search can highlight the benefits of each method. Finally, other methods for clustering or subdi-

viding PLM embeddings should be considered and tested. We expect advances in LLM capabilities and more advanced protein representations may drive further improvement on these tasks, and hope this framework can provide a useful proof-of-concept as this field develops further.

Code availability

Code is available at https://github.com/ElanaPearl/interp-agents

Impact Statement

This paper presents work whose goal is to advance the field of protein annotation. There are many potential societal consequences of our work, such as helping biologists better understand and annotate novel features, or discover new functional domains in proteins. We do not see significant or specific ethical risks with this work, though we suppose it is possible that better understanding (and eventually designing) proteins could be used maliciously in rare circumstances.

Acknowledgments

The authors wish to thank Wei Deng, Jessica Karaguesian, Brian Trippe, and Ben Viggiano for helpful conversations that improved this work. JS is supported by the Arc Institute. ES is supported by NSF GRFP grant DGE-2146755.

References

Adams, E., Bai, L., Lee, M., Yu, Y., and AlQuraishi, M. From mechanistic interpretability to mechanistic biology: Training, evaluating, and interpreting sparse autoencoders on protein language models. *bioRxiv*, pp. 2025–02, 2025.

Baltoumas, F. A., Karatzas, E., Liu, S., Ovchinnikov, S., Sofianatos, Y., Chen, I.-M., Kyrpides, N. C., and Pavlopoulos, G. A. Nmpfamsdb: a database of novel protein families from microbial metagenomes and metatranscriptomes. *Nucleic Acids Research*, 52(D1):D502–D512, 2024.

Bateman, A., Coin, L., Durbin, R., Finn, R. D., Hollich, V., Griffiths-Jones, S., Khanna, A., Marshall, M., Moxon, S., Sonnhammer, E. L., et al. The pfam protein families database. *Nucleic acids research*, 32(suppl_1):D138–D141, 2004.

Buchan, D. W., Shepherd, A. J., Lee, D., Pearl, F. M., Rison, S. C., Thornton, J. M., and Orengo, C. A. Gene3d: structural assignment for whole genes and genomes using the cath domain structure database. *Genome research*, 12(3): 503–514, 2002.

Carugo, O. and Pongor, S. A normalized root-mean-spuare distance for comparing protein three-dimensional structures. *Protein science*, 10(7):1470–1473, 2001.

Consortium, U. Uniprot: a hub for protein information. *Nucleic acids research*, 43(D1):D204–D212, 2015.

Cosgriff, A. J. and Pittard, A. A topological model for the general aromatic amino acid permease, arop, of escherichia coli. *Journal of bacteriology*, 179(10):3317–3323, 1997.

Hunter, S., Apweiler, R., Attwood, T. K., Bairoch, A., Bateman, A., Binns, D., Bork, P., Das, U., Daugherty, L., Duquenne, L., et al. Interpro: the integrative protein signature database. *Nucleic acids research*, 37(suppl_1): D211–D215, 2009.

Jones, P., Binns, D., Chang, H.-Y., Fraser, M., Li, W., McAnulla, C., McWilliam, H., Maslen, J., Mitchell, A., Nuka, G., et al. Interproscan 5: genome-scale protein function classification. *Bioinformatics*, 30(9):1236–1240, 2014.

Jumper, J., Evans, R., Pritzel, A., Green, T., Figurnov, M., Ronneberger, O., Tunyasuvunakool, K., Bates, R., Žídek, A., Potapenko, A., et al. Highly accurate protein structure prediction with alphafold. *nature*, 596(7873):583–589, 2021.

Kandathil, S. M., Lau, A. M., Buchan, D. W., and Jones, D. T. Foldclass and merizo-search: Scalable structural similarity search for single-and multi-domain proteins using geometric learning. *Bioinformatics*, pp. btaf277, 2025.

Karin, E. L. and Steinegger, M. Cutting edge deep-learning based tools for metagenomic research. *National Science Review*, pp. nwaf056, 2025.

Lau, A. M., Kandathil, S. M., and Jones, D. T. Merizo: a rapid and accurate protein domain segmentation method using invariant point attention. *Nature Communications*, 14(1):8445, 2023.

Lau, A. M., Bordin, N., Kandathil, S. M., Sillitoe, I., Waman, V. P., Wells, J., Orengo, C. A., and Jones, D. T. Exploring structural diversity across the protein universe with the encyclopedia of domains. *Science*, 386(6721):eadq4946, 2024.

Lin, Z., Akin, H., Rao, R., Hie, B., Zhu, Z., Lu, W., Smetanin, N., Verkuil, R., Kabeli, O., Shmueli, Y., et al. Evolutionary-scale prediction of atomic-level protein structure with a language model. *Science*, 379(6637): 1123–1130, 2023.

Orengo, C. A., Michie, A. D., Jones, S., Jones, D. T., Swindells, M. B., and Thornton, J. M. Cath–a hierarchic classification of protein domain structures. *Structure*, 5(8):1093–1109, 1997.

Raba, M., Dunkel, S., Hilger, D., Lipiszko, K., Polyhach, Y., Jeschke, G., Bracher, S., Klare, J. P., Quick, M., Jung, H., et al. Extracellular loop 4 of the proline transporter putp controls the periplasmic entrance to ligand binding sites. *Structure*, 22(5):769–780, 2014.

Shindyalov, I. N. and Bourne, P. E. Protein structure alignment by incremental combinatorial extension (ce) of the optimal path. *Protein engineering*, 11(9):739–747, 1998.

Simon, E. and Zou, J. Interplm: Discovering interpretable features in protein language models via sparse autoencoders. *bioRxiv*, pp. 2024–11, 2024.

Templeton, A., Conerly, T., Marcus, J., Lindsey, J., Bricken, T., Chen, B., Pearce, A., Citro, C., Ameisen, E., Jones, A., Cunningham, H., Turner, N. L., McDougall, C., MacDiarmid, M., Tamkin, A., Durmus, E., Hume, T., Mosconi, F., Freeman, C. D., Sumers, T. R., Rees, E., Batson, J., Jermyn, A., Carter, S., Olah, C., and Henighan, T. Scaling monosemanticity: Extracting interpretable features from claude 3 sonnet, 2024. URL https://transformer-circuits.pub/2024/scaling-monosemanticity/. Accessed: July 7, 2025.

van Kempen, M., Kim, S. S., Tumescheit, C., Mirdita, M., Gilchrist, C. L., Söding, J., and Steinegger, M. Foldseek: fast and accurate protein structure search. *Biorxiv*, pp. 2022–02, 2022.

Zhang, Y. and Skolnick, J. Tm-align: a protein structure alignment algorithm based on the tm-score. *Nucleic acids research*, 33(7):2302–2309, 2005.

A. Flexible regions

We note that many features still have a high code-based F1 even though they also have high $RMSD_{100}$. Some of these are regions that are structurally flexible, for example f/73 below. We show three proteins, each with a homeodomain-like region highlight in orange and blue, and the highly activated region for f/73 in pink.

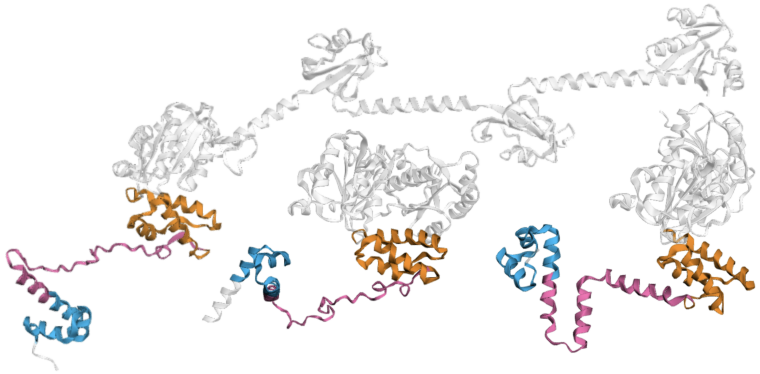

Figure 1. f/73 captures a variety of structures that all link two structurally consistent domains. Here, three proteins have homeolike-domains are in orange and blue, while the highly active region for f/73 is in pink

B. Understanding granular features

For six features, we used o4-mini-high to attempt to find citations that discussed the specific regions of interest. An example prompt is given below, followed by the best citation (where applicable) found by the model. Each citation returned by the model was reviewed manually, as the model could sometimes hallucinate specific quotes or mutations that were not found in the underlying papers. Where no relevant citation was retrieved, the feature was analyzed manually to determine its specific function. Sometimes very promising literature about the specific region exists, but was not returned by o4-mini-high, perhaps because of only asking about 10 gene-species combinations per feature. For example, manually searching for additional papers revealed that f/253 corresponds to the cytoplasmic loop between transmembrane domain 2 and 3 in a topological model of amino acid permeases (Cosgriff & Pittard, 1997).

Prompt for f/515

What do we know about the following proteins in these amino acid regions mentioned for each? Cite papers that look specifically at or very near these regions
ACTP_PECCP Cation/acetate symporter ActP (Acetate permease) (Acetate transporter ActP) in Pectobacterium carotovorum subsp. carotovorum (strain PC1) at 332
MNTH_AGRFC Divalent metal cation transporter MntH in Agrobacterium fabrum (strain C58 / ATCC 33970) (Agrobacterium tumefaciens (strain C58)) at 309
...
KUP_CYTH3 Probable potassium transport system protein Kup in Cytophaga hutchinsonii (strain ATCC 33406 / DSM 1761 / CIP 103989 / NBRC 15051 / NCIMB 9469 / D465) at 271
KUP_STRA1 Probable potassium transport system protein Kup in Streptococcus agalactiae serotype Ia (strain ATCC 27591 / A909 / CDC SS700) at 277
PUTP_STAAN Sodium/proline symporter (Proline permease) in Staphylococcus aureus (strain N315) at 310
In total (across all proteins) provide me only with 2-4 of the best matching citations and what we know about the region from each paper

Table 1. o4-retrieved feature citations for specific sub-domains.

Feature	o4 description of best citation	Paper link
73	No citation retrieved discussed this specific subdomain (a flexible linker region sandwiched between HTH domains).	—
253	No citation retrieved discussed this specific subdomain (in the cytoplasmic loop between TM2 and TM3).	—
401	"Schmidt *et al.* solved crystal structures of the *Aquifex aeolicus* Kdo transferase (WaaA), a GT–B family homolog, revealing that the loop encompassing residues 98–102 (equivalent to *E. coli* position ∼101) shapes the acceptor–substrate binding site…"	https://pubmed.ncbi.nlm.nih.gov/22474366/
515	"Site-directed mutagenesis targeting extracellular loop 4 of *S. aureus* PutP (residues 310, 314, 318) showed that altering the amino acid at position 310 completely abolishes proline uptake…"	https://www.sciencedirect.com/science/article/pii/S0969212614000835?utm_source=chatgpt.com
711	"In vivo cysteine cross-linking between TM2 and TM8—including sites around residue 316—demonstrated that MurJ adopts both inward- and outward-facing states during transport. Disruption of membrane potential selectively destabilized the inward-facing conformation..."	https://pubmed.ncbi.nlm.nih.gov/30482840/
931	"Residue 88 (human numbering) lies in the β-strand F of the TTR fold, forming part of a critical hydrogen-bond network that stabilizes the tetramer…"	https://pmc.ncbi.nlm.nih.gov/articles/PMC8122960/

C. Missing CATH annotations

Below we show the first 100 missing CATH annotations identified by our workflow, of the 491 that match with TED annotations. We considered a match if TED contained a code that was within the same topology as the top CATH code for a given feature. Best code represents the top CATH code for that feature, while TED label is the exact TED label for that protein (which may either be a CATH homologous superfamily or topology).

Table 2. Rows 1–50

Protein	Feature	Best code	TED label
Q01473	4	1.20.120.160	1.20.120
Q7Y0V9	52	3.30.530.20	3.30.530.20
Q0WV12	52	3.30.530.20	3.30.530.20
Q9FVI6	52	3.30.530.20	3.30.530.20
Q8XA02	57	3.10.105.10	3.10.105.10
P46890	57	3.10.105.10	3.10.105.10
P77172	81	3.30.70.270	3.30.70.270
Q58121	112	1.20.58.340	1.20.58
O28044	112	1.20.58.340	1.20.58
Q01473	119	1.20.120.160	1.20.120
Q49430	121	1.20.1560.10	1.20.1560.10
Q0VFX2	129	1.20.5.500	1.20.5
Q5BL57	129	1.20.5.500	1.20.5
Q499U4	129	1.20.5.500	1.20.5
Q25C79	129	1.20.5.500	1.20.5
Q4UMJ9	159	1.20.1250.20	1.20.1250.20
P28246	159	1.20.1250.20	1.20.1250.20
Q9JXM5	169	1.25.40.10	1.25.40.10
O51072	180	1.25.40.10	1.25.40.10
Q8K4P7	180	1.25.40.10	1.25.40.10
Q8RWN0	194	3.40.395.10	3.40.395.10
Q0WKV8	194	3.40.395.10	3.40.395.10
Q09275	194	3.40.395.10	3.40.395.10
O13769	194	3.40.395.10	3.40.395.10
Q8L7S0	194	3.40.395.10	3.40.395.10
Q2PS26	194	3.40.395.10	3.40.395.10
Q54KW6	196	1.25.40.10	1.25.40
P34511	218	1.25.40.20	1.25.40.20
P18540	251	3.40.50.2300	3.40.50.2300
O22232	281	3.80.10.10	3.80.10
O04615	310	2.60.210.10	2.60.210.10
Q9FKD7	310	2.60.210.10	2.60.210.10
Q9XHZ8	310	2.60.210.10	2.60.210.10
Q8C008	371	2.60.40.10	2.60.40
Q9STL8	399	3.40.140.10	3.40.140.10
Q9FG71	399	3.40.140.10	3.40.140.10
O82264	399	3.40.140.10	3.40.140.10
Q9LYC2	399	3.40.140.10	3.40.140.10
Q04368	399	3.40.140.10	3.40.140.10
P76349	401	3.40.50.2000	3.40.50.2000
D3DJ42	401	3.40.50.2000	3.40.50.20
Q5WSK6	401	3.40.50.2000	3.40.50.2000
Q9SH31	419	3.40.50.2000	3.40.50
Q3E9A4	419	3.40.50.2000	3.40.50.2000
Q9LFP3	434	3.40.50.2000	3.40.50.2000
P75207	442	1.20.1560.10	1.20.1560.10
Q49430	443	1.20.1560.10	1.20.1560.10
Q9ZD06	449	3.30.2350.10	3.30.2350.10
Q8FB47	449	3.30.2350.10	3.30.2350.10
Q8ZGM2	449	3.30.2350.10	3.30.2350.10

Table 3. Rows 51–100

Protein	Feature	Best code	TED label
Q92HG4	449	3.30.2350.10	3.30.2350.10
P77607	544	3.40.50.1390	3.40.50.1390
Q8XA02	607	3.10.105.10	3.10.105.10
P46890	607	3.10.105.10	3.10.105.10
A9NCA7	713	3.40.50.2000	3.40.50.2000
O67214	713	3.40.50.2000	3.40.50.2000
P37597	751	1.20.1250.20	1.20.1250.20
O04292	789	3.30.450.20	3.30.450.20
Q9Z7F1	789	3.30.450.20	3.30.450.20
A2XBL9	789	3.30.450.20	3.30.450.20
Q39123	789	3.30.450.20	3.30.450.20
B0K165	843	3.30.479.30	3.30.479.30
P32233	848	3.40.50.300	3.40.50.300
Q2NL82	848	3.40.50.300	3.40.50.300
A0A0H2URH2	849	3.40.50.2000	3.40.50.2000
A0A0H2URJ6	849	3.40.50.2000	3.40.50.2000
P33694	849	3.40.50.2000	3.40.50.2000
A1JSF2	873	3.40.50.300	3.40.50.300
P50837	889	3.30.420.10	3.30.420.10
Q60953	889	3.30.420.10	3.30.420.10
P53296	891	3.30.559.10	3.30.559.30
I1S097	894	3.90.550.10	3.90.550.10
D3ZZN9	936	2.60.40.150	2.60.40.150
Q9C8E6	936	2.60.40.150	2.60.40.150
P54739	972	3.30.200.20	3.30.200.20
P54735	972	3.30.200.20	3.30.200.20
C4JDF8	1003	1.10.1200.10	1.10.1200.10
P39404	1013	3.40.50.2300	3.40.50.2300
O83933	1016	1.20.1600.10	1.20.1600
P63400	1039	1.10.1760.20	1.10.1760
O67248	1039	1.10.1760.20	1.10.1760
Q58299	1053	3.60.40.10	3.60.40.10
O29259	1119	1.10.443.10	1.10.443.10
P07261	1119	1.10.443.10	1.10.443.20
O83202	1205	3.30.70.270	3.30.70.270
P77172	1205	3.30.70.270	3.30.70.270
Q2NKC0	1205	3.30.70.270	3.30.70.270
Q10419	1233	2.40.30.170	2.40.30.170
P55501	1239	3.30.420.10	3.30.420.10
Q44493	1320	2.150.10.10	2.150.10.10
P75800	1329	3.30.70.1230	3.30.70.270
B5XZP2	1347	1.20.1250.20	1.20.1250.20
D0CCT2	1347	1.20.1250.20	1.20.1250.20
E0T2N0	1347	1.20.1250.20	1.20.1250.20
O34353	1360	2.120.10.80	2.120.10.30
Q10412	1380	1.20.920.10	1.20.920
Q6YRK2	1416	3.30.70.270	3.30.70.270
B0XZV4	1447	1.20.1250.20	1.20.1250.20
O83837	1466	1.25.40.10	1.25.40
Q8IAR5	1482	2.30.42.10	2.30.42.10